EXOSKELETONS

A portable inflatable soft wearable robot to assist the shoulder during industrial work

Yu Meng Zhou†, Cameron J. Hohimer†, Harrison T. Young‡, Connor M. McCann‡, David Pont-Esteban‡, Umut S. Civici, Yichu Jin, Patrick Murphy, Diana Wagner, Tazzy Cole, Nathan Phipps, Haedo Cho, Franchesco Bertacchi, Isabella Pignataro, Tommaso Proietti, Conor J. Walsh*

Repetitive overhead tasks during factory work can cause shoulder injuries resulting in impaired health and productivity loss. Soft wearable upper extremity robots have the potential to be effective injury prevention tools with minimal restrictions using soft materials and active controls. We present the design and evaluation of a portable inflatable shoulder wearable robot for assisting industrial workers during shoulder-elevated tasks. The robot is worn like a shirt with integrated textile pneumatic actuators, inertial measurement units, and a portable actuation unit. It can provide up to 6.6 newton-meters of torque to support the shoulder and cycle assistance on and off at six times per minute. From human participant evaluations during simulated industrial tasks, the robot reduced agonist muscle activities (anterior, middle, and posterior deltoids and biceps brachii) by up to 40% with slight changes in joint angles of less than 7% range of motion while not increasing antagonistic muscle activity (latissimus dorsi) in current sample size. Comparison of controller parameters further highlighted that higher assistance magnitude and earlier assistance timing resulted in statistically significant muscle activity reductions. During a task circuit with dynamic transitions among the tasks, the kinematics-based controller of the robot showed robustness to misinflations (96% true negative rate and 91% true positive rate), indicating minimal disturbances to the user when assistance was not required. A preliminary evaluation of a pressure modulation profile also highlighted a trade-off between user perception and hardware demands. Finally, five automotive factory workers used the robot in a pilot manufacturing area and provided feedback.

INTRODUCTION

Work-related musculoskeletal disorders are a major problem in the workforce, accounting for nearly 70 million physician visits in the United States per year (*1*). This high injury risk is associated with the high demands in many labor-intensive industries [workers may lift their arms an average of 4600 times each day during automotive assembly (*2*)]. In 2020, 63,100 workplace shoulder injuries (*3*) resulted in a median of 25 to 37 days away from work (*4*), resulting in productivity loss and high costs. Automation technologies and ergonomic interventions, such as lift assist devices, can reduce the risk of injuries; however, they often require modification of the factory line and are thus expensive to implement and hard to generalize to multiple tasks. Wearable devices, such as passive shoulder supports and exoskeletons, have the potential to be more versatile by supporting the worker directly and to be more seamlessly integrated within an existing work environment.

Most wearable shoulder assistive devices for industrial work are made with rigid components and use passive actuation such as spring-based mechanisms (example devices include Levitate Airframe, Ekso Bionics Evo, Hilti Exo-01, Ottobock Paexo, and Skelex 360-XFR). With a lighter structure than their active counterparts, these exoskeletons have shown the ability to reduce upper extremity agonistic muscle activation between 16 and 73% for a range of activities, including holding, pointing, and reaching (*5*–*8*), with larger reductions observed with greater assistance levels (*9*).

However, increased antagonistic muscle activities with some passive shoulder exoskeletons have also been observed (*8*, *10*–*12*). From a review of seven spring-based exoskeletons, muscle activity increases between 25% and 107% were found (*8*). Although these increases are not observed in all designs, it is a common challenge to tackle for passive exoskeletons, often because of the need to move against the assistance to lower the arm. There also exists a trade-off between assistance and resistance for passive exoskeletons because greater assistance has been shown to reduce muscle activation during desired working periods (*10*, *13*) but is associated with increased resistance and discomfort (*10*, *14*), which may be especially highlighted for dynamic tasks. Passive exoskeletons present this challenge of selecting optimal support settings to allow suitable assistance without imposing adverse effects (*8*).

Soft active robots, on the other hand, combine the benefits of controllable actuation with more compact size and lower weight on the targeted limbs because of the use of soft materials. Additionally, active actuation has the potential to overcome the challenge of assistance and resistance trade-off because it may provide assistance when needed and power off to minimize resistance otherwise. When powered off, soft active robots have been shown to offer mechanical transparency, exerting minimal restrictions on the user's natural range of motion (*15*). So far, soft active robots have been primarily designed for medical applications, with initial validations on healthy individuals performing activities of daily living. Specifically, preliminary evaluations of inflatable shoulder robots during shoulder abduction and flexion showed reductions in deltoid activation up to 70% (*16*, *17*), whereas cable-driven robots reduced deltoid

John A. Paulson School of Engineering and Applied Sciences, Harvard University, Cambridge, MA, USA.
*Corresponding author. Email: walsh@seas.harvard.edu
†These authors contributed equally to this work.
‡These authors contributed equally to this work.

activity up to 42% when lifting up to 1 kg of weight (*18*). Recently, a portable inflatable shoulder robot demonstrated assistance for individuals with amyotrophic lateral sclerosis (ALS) (*15*), resolving a key limitation of portability for inflatable robots (*19*). Although most validations are under constrained nonfunctional conditions, the progress of these soft active systems suggests their potential to assist in different underexplored applications, such as industrial work.

Here, we present the design and evaluation of a portable soft inflatable robot for shoulder assistance suitable for assisting shoulder-elevated industrial tasks. Expanding on our previous work (*13*, *16*, *20*–*22*), we designed a portable actuation unit to enable untethered use. Moreover, to improve usability, we integrated all actuation, sensing, and textile components into functional apparel. We used a previously demonstrated kinematics state-machine controller (*20*) and extended its evaluation through experimental simulation of common tasks in industrial settings. Additionally, we compared different assistance timings and actuator pressures to understand the effects of varying control parameters on the wearer's muscle activity and biomechanics. To evaluate the performance of the robot, we conducted three experiments with individuals performing shoulder-elevated tasks and analyzed user kinematics, muscle activity, and accuracy of the controller. To further demonstrate the capabilities of an active robot, we performed a preliminary comparison between fixed and modulated assistance during a dynamic holding task and evaluated user preference in addition to biomechanics. As a final proof of concept, the robot was used by five workers in an automotive pilot manufacturing area. Qualitative feedback on their experience using the robot during real industrial tasks was collected.

RESULTS

Soft wearable shoulder robot and characterization

We designed a portable soft wearable shoulder robot with textile inflatable actuators, inertial measurement units (IMUs) for sensing kinematics, and a portable actuation unit all integrated into custom apparel (Fig. 1A and fig. S1). To quantify the range of assistance levels delivered by the robot, we used a custom torque measurement apparatus (*23*) (Supplementary Methods). The robot was able to provide 6.8 Nm of torque for a representative pose of overhead work (shoulder elevated at 80°) at 100 kPa (fig. S5).

To assess whether the robot could assist during controlled and dynamic tasks indicative of industrial use, we conducted experiments involving simulated factory tasks requiring shoulder elevation motion. Specifically, we conducted three experiments: holding with various assistance magnitudes (low, med, high) (Fig. 1B), drilling with various assistance timings (early, mid, late) (Fig. 1C), and a circuit task with elevated shoulder tasks and other transition tasks not requiring assistance (Fig. 1D). The objective of these experiments was also to understand the effect of assistance parameters on kinematics and muscle activity. Additionally, to further explore the capabilities of an active robot, we performed a preliminary demonstration of providing modulated assistance (mod) (Fig. 1E, Supplementary Methods, and fig. S7).

All experiments were conducted with and without the robot, denoted as exo and no exo conditions, respectively, and with specific assistance conditions during exo for holding, drilling, and pressure modulation experiments (Fig. 1, B, C, and E). We measured upper extremity kinematics and electromyography (EMG) from five muscle groups—anterior deltoid (AD), middle deltoid (MD), posterior deltoid (PD), biceps brachii (BIC), and latissimus dorsi (LAT)—on both sides of the body. PD, MD, AD, and BIC were measured because shoulder flexion, abduction, and elbow flexion and extension are common in the experiment tasks. BIC, in addition to powering elbow flexion, also acts as a stabilizer during shoulder elevation (*24*). LAT is an antagonistic muscle responsible for shoulder adduction and extension (*25*) and was used to assess the hindrance of the robot.

Data from nine and eight individuals were analyzed for the holding and drilling experiments, respectively, five individuals for the circuit experiment, and four individuals for the pressure modulation experiment. The total participant pool included five females and nine males, one left dominant, with weight of 73 ± 15 kg (mean ± SD) and height of 1.7 ± 0.1 m across all participants (table S1).

Reduced muscle activity during holding task

To assess user biomechanics during a constrained weighted motion and the effect of assistance magnitude, the holding experiment involved holding a 4-kg weight at approximately eye level for three repetitions of 30 s. The baseline assistance pressure, low, was individualized on the basis of user-perceived support (denoted as P*), and med and high were increased 16 and 32 kPa, respectively, from the low pressure.

During the holding experiment, statistically significant reductions in mean EMG across PD, MD, and BIC were found during high and med conditions, AD for high condition, and LAT during all conditions [Friedman's test with Tukey-Kramer post hoc analysis, $n = 27$ (nine participants, three repetitions), $P < 0.05$] (Fig. 2A). Greater mean percentage EMG reductions were observed at higher assistance magnitudes for PD, MD, and BIC, but no statistical significance was found among the various assistance conditions. AD, the most activated muscle during the hold, experienced mean reductions of 29% at high magnitude, and the highest absolute reduction of 4.8% MVC (maximum voluntary contraction) ($P < 0.01$). LAT was activated at 7% MVC during the no exo condition (Fig. 2A) and was assisted with more than 30% EMG reduction, or 2.2% MVC, across all assistance magnitudes ($P < 0.01$) (Fig. 2A).

Changes in kinematics during holding task

No significant differences in kinematics were found across the three assistance magnitudes [Friedman's test with Tukey-Kramer post hoc analysis, $n = 18$ (nine participants, two repetitions), $P > 0.05$] (Fig. 2B) during the holding experiment, whereas differences were observed between no exo and exo conditions ($P < 0.05$). Specifically, at med and high assistance levels, statistically significant increases in elevation angles were 10.1° and 9.6°, respectively ($P < 0.05$). Shoulder horizontal extension angles were also increased by 10.0°, 10.4°, and 11.4°, respectively, for the low, med, and high conditions ($P < 0.01$). Considering normalized segment lengths to anthropometric averages (*26*, *27*), these changes correspond to the elbow being 5.3 cm more lateral, 4.3 cm more cranial, and 0.4 cm more posterior while using the robot (average of all exo conditions) (Fig. 2C).

Reduced muscle activity during drilling task

To evaluate user biomechanics during a functional task and to assess the effects of assistance timing, the drilling experiment required participants to drill with one hand a 10-cm bolt in and out for 10 cycles at individualized heights with resulting shoulder elevation at 84.9° ± 5.3° (fig. S2). The various assistance timings were determined by the

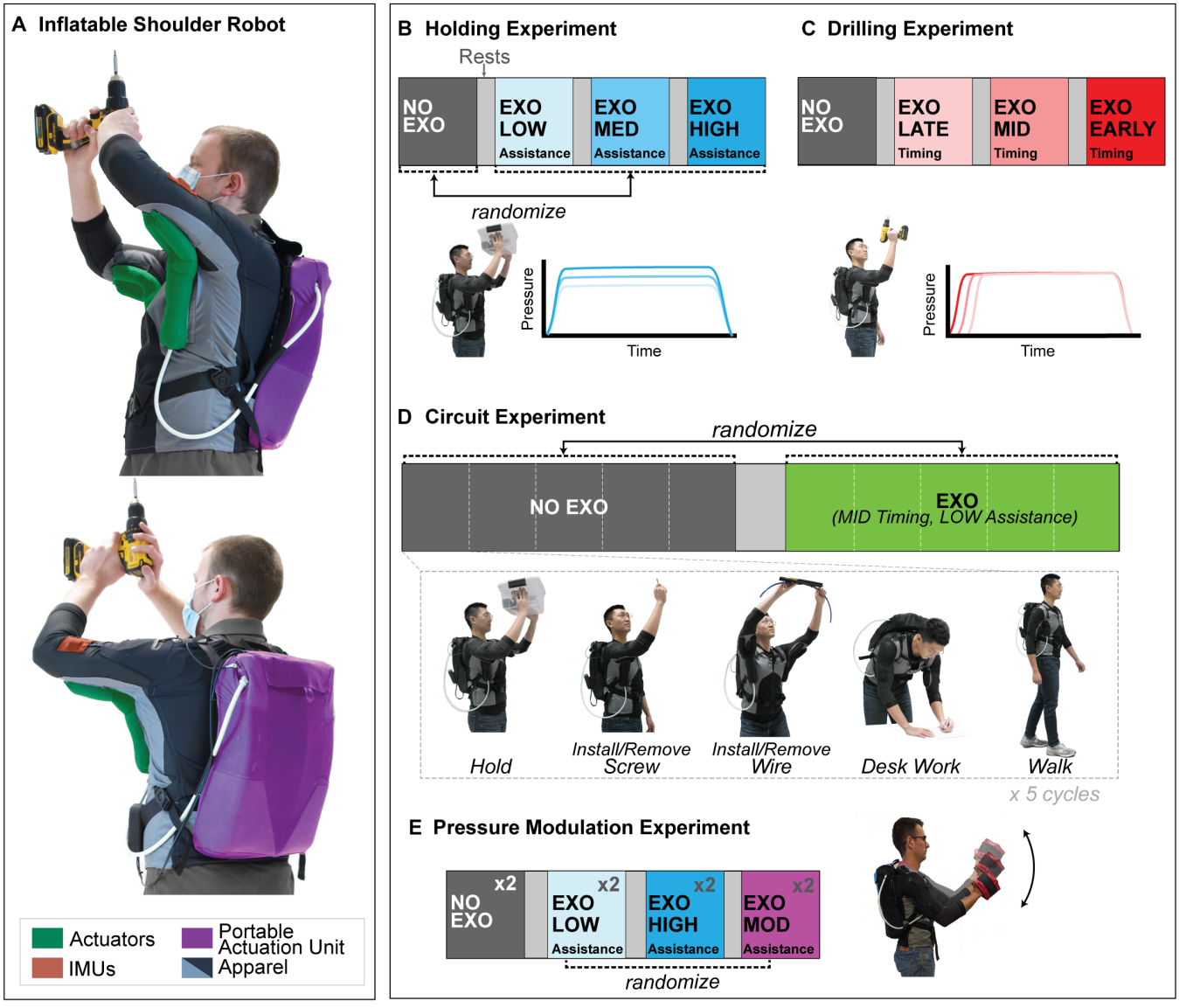

Fig. 1. Inflatable shoulder wearable robot and experimental methods. (**A**) Soft inflatable shoulder wearable robot with portable actuation unit, textile-based inflatable actuators, and IMUs. Experimental methods, including (**B**) holding experiment with three assistance magnitudes, (**C**) drilling experiment with three assistance timings, (**D**) circuit experiment involving a sequence of tasks requiring and not requiring assistance, and (**E**) pressure modulation experiment.

controller onset angle (θ_{on}), which is the elevation angle (IMU-estimated) at which the robot starts inflating (fig. S1C). The early, mid, and late conditions were set to 45°, 55°, and 65° onset angles, respectively, with the resulting IMU-estimated onset angles being 47.00 ± 2.40°, 54.48 ± 0.29°, and 64.63 ± 0.28°, respectively.

During the arm raising and drilling portions of the drilling task, statistically significant EMG reductions were observed for PD and MD during the early assistance timing [Friedman's test with Tukey-Kramer post hoc analysis, $n = 24$ (eight participants, three repetitions), $P < 0.01$ and $P < 0.05$, respectively] (Fig. 3A). Specifically, PD and MD reduced muscle activation by 39% and 30%, respectively, as compared with no exo. No statistically significant differences in muscle activity were observed among the assistance timings.

Late inflation leads to fewer kinematic deviations during drilling task

With the robot on, at the initial bolt touch position, the shoulder was 8.6°, 7.9°, and 7.3° more elevated for early, mid, and late assistance timings, respectively, as compared with the no exo condition (Fig. 3B) [Friedman's test with Tukey-Kramer post hoc analysis, $n = 24$ (eight participants, three repetitions), $P < 0.05$ for late, $P < 0.01$ for mid and early], whereas no significant differences were found among the exo conditions. The shoulder horizontal extension and elbow angles were not significantly different when using the robot. These changes in shoulder elevation resulted in the elbow position being more lateral (Fig. 3C). Assuming segment lengths of anthropometric averages (*26*, *27*) for all participants, we observed

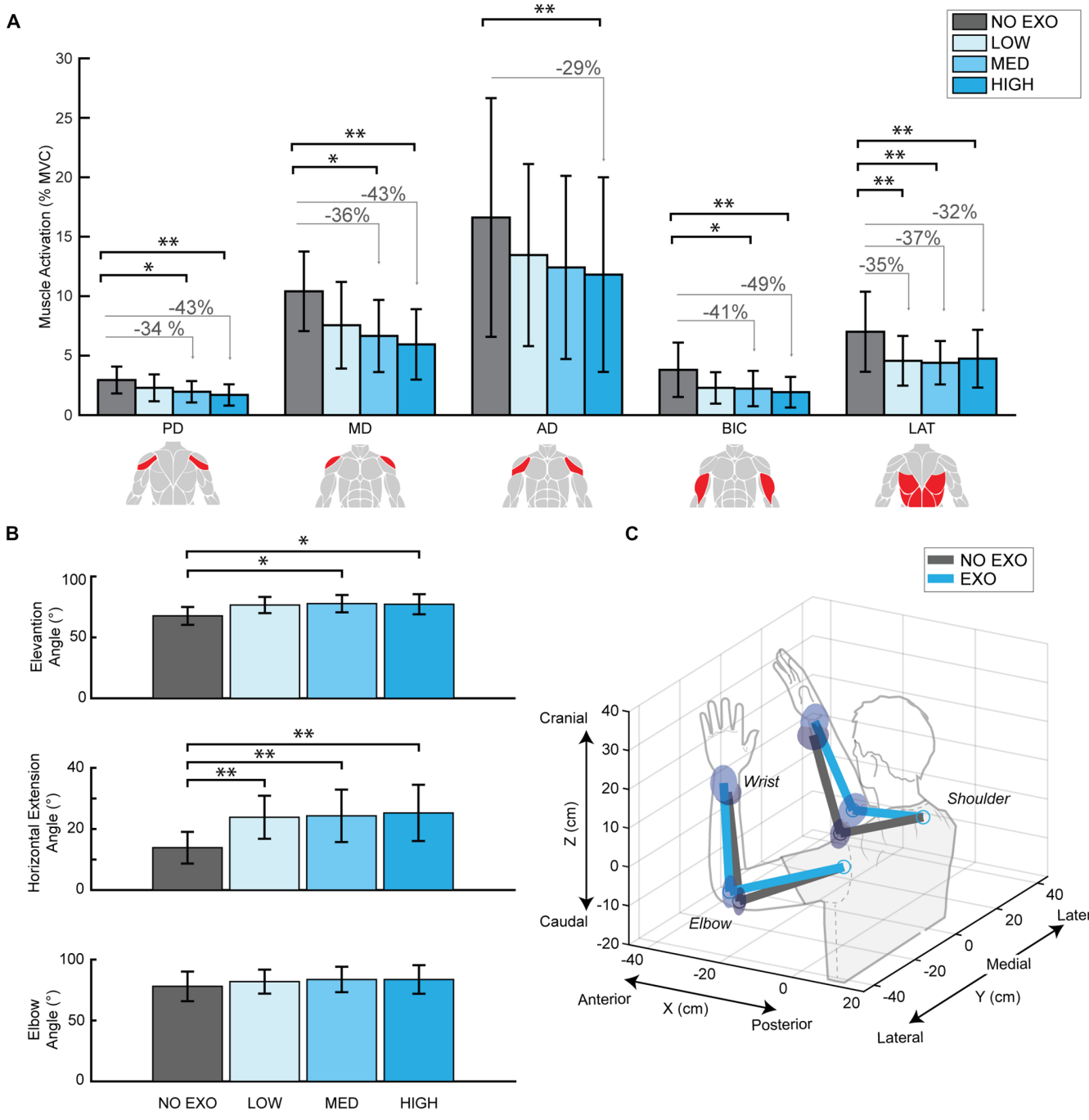

Fig. 2. Holding experiment results. (**A**) EMG measurements in % MVC for no exo, low, med, and high conditions for all muscle groups during the static holding period. The error bars represent SDs across hold repetitions of all participants [significant differences from Friedman's test with Tukey-Kramer post hoc analysis are indicated with $*P < 0.05$ and $**P < 0.01$, $n = 27$ (nine participants, three conditions)]. (**B**) Joint angles during the holding period for all conditions showing shoulder elevation, horizontal extension, and elbow angles. The error bars represent SDs across hold repetitions of all participants [significant differences from Friedman's test with Tukey-Kramer post hoc analysis are indicated with $*P < 0.05$ and $**P < 0.01$, $n = 18$ (nine participants, two conditions)]. (**C**) Holding kinematics illustrating the normalized positions of shoulder acromion, elbow, and wrist joint center positions for exo (blue) (averaged across low, med, and high) and no exo conditions (black). The ellipsoids indicate the corresponding position SDs across participants, with the length of the principal axes of the ellipsoids being the SDs in each direction (*X*, anterior-posterior; *Y*, medial-lateral; *Z*, caudal-cranial).

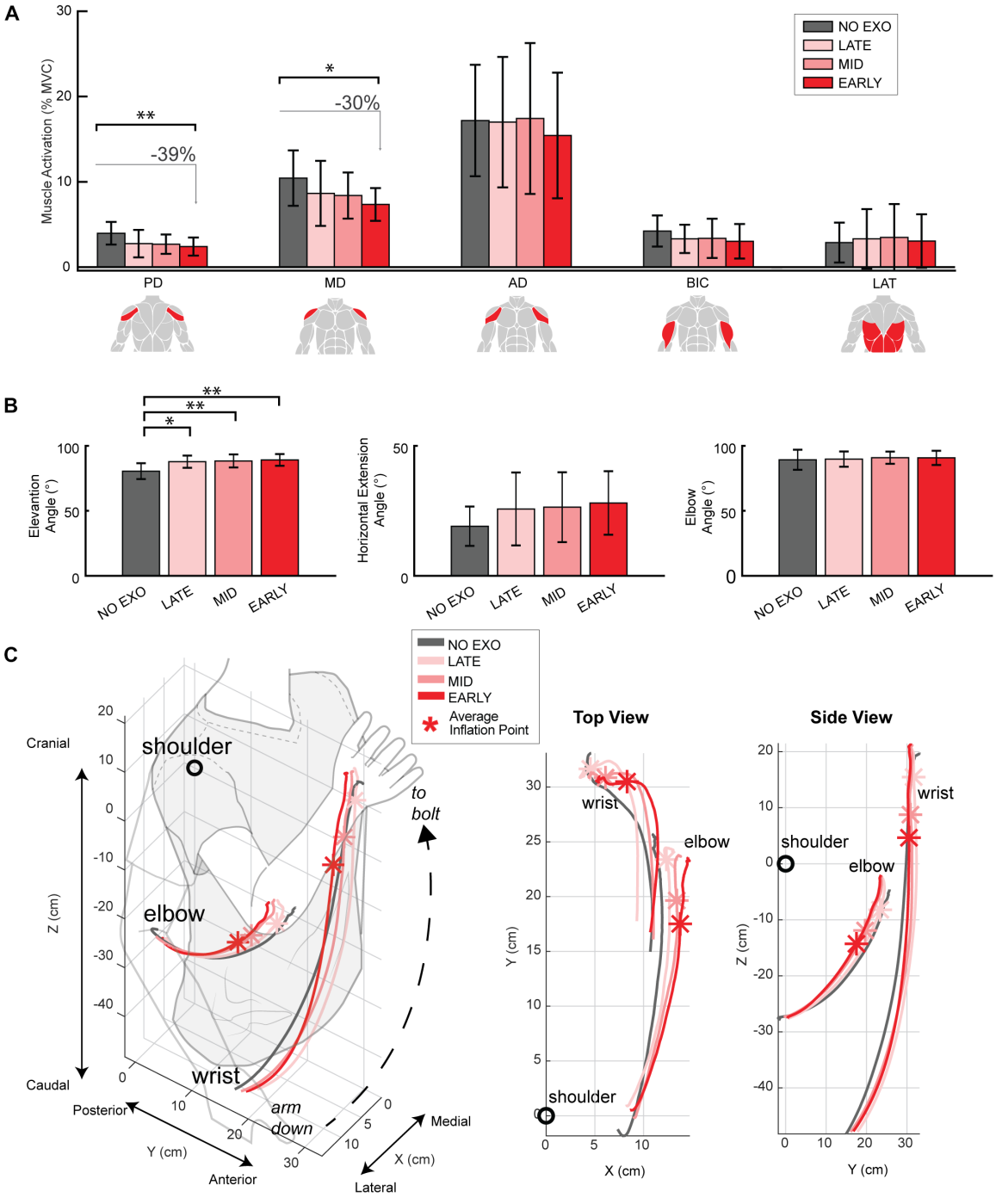

Fig. 3. Drilling experiment results. (**A**) EMG measurements in % MVC for no exo, early, mid, and late conditions for all muscle groups during the arm raising and drilling phases of the task (three cycles drilling out direction for each participant). The error bars represent SDs across drill repetitions of all participants. (**B**) Joint angles at the initial bolt touch position for no exo, early, mid, and late conditions showing shoulder elevation, horizontal extension, and elbow angles. The error bars represent SDs across drill repetitions of all participants. For (A) and (B), significant differences from Friedman's test with Tukey-Kramer post hoc analysis are indicated with $*P < 0.05$ and $**P < 0.01$, $n = 24$ (eight participants, three repetitions). (**C**) Drilling experiment elbow and wrist center trajectories when targeting the bolt for early, mid, and late assistance timings and no exo condition using segment lengths normalized to anthropometrics averages and averaged across participants. The average inflation point (normalized time and position) is marked by the asterisk for each exo condition.

that the average elbow trajectory was more lateral for early assistance timing compared with late, with a difference of the maximum average lateral positions of 1.6 cm or approximately 36% of total elbow lateral motion during the no exo condition.

Muscle activity reduction and kinematic changes during circuit task

The objective of the third experiment was to evaluate the robot in a more realistic and dynamic circuit task, involving higher angles and various movement speeds, and to understand whether the system could assist when needed and not impede during transitions or when not required. The circuit experiment consisted of five cycles of three shoulder-elevated tasks—holding (holding 4 kg for 20 s), manual screw installation (alternating installation and removal of four screws at different heights), and hose wiring (alternating installation and removal)—and two tasks not requiring assistance—desk work involving writing on paper and walking.

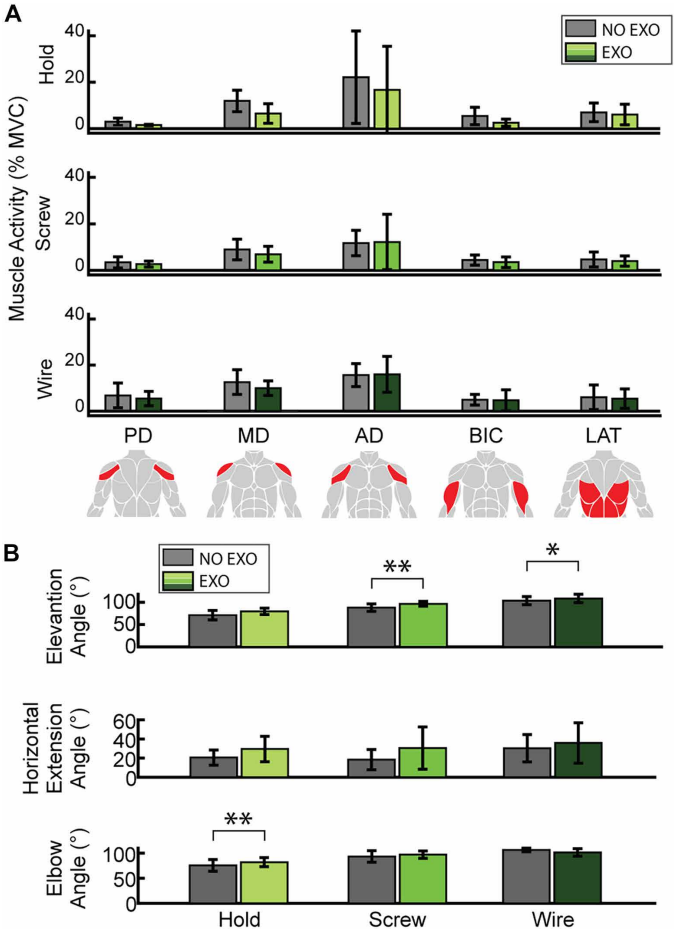

Fig. 4. Circuit experiment results. (**A**) EMG measurements in % MVC for no exo and exo conditions for all muscle groups during each circuit task during periods of elevated work. The error bars represent SDs across participants (no significant differences were found with paired *t* test for comparing normal data and Wilcoxon's signed-rank test for comparing non-normal data, with normality determined by Shapiro-Wilk parametric hypothesis test, $n = 5$). (**B**) Joint angle comparisons between exo and no exo conditions showing differences in shoulder elevation, horizontal extension, and elbow angles during screw task and elevation angle during wiring task. The error bars represent SDs across participants (significant differences from paired *t* test for comparing normal data and Wilcoxon's signed-rank test for comparing non-normal data, with normality determined by Shapiro-Wilk parametric hypothesis test, are indicated with $*P < 0.05$ and $**P < 0.01$, $n = 5$).

For all the agonist muscle groups during the holding task and for PD and MD during screw and wiring tasks, reduced mean muscle activity was found but without statistical significance (Fig. 4A) (paired *t* test for normal data and Wilcoxon's signed-rank test for non-normal data, $n = 5$, $P > 0.05$). For all tasks, we observed no significant increase in LAT activation (Fig. 4A). Comparing the results for the holding task performed in isolation to the part of the circuit experiment, there were no differences in the absolute EMG reductions in the agonist muscle groups [Mann-Whitney-Wilcoxon test, $n = 9$ for holding experiment, $n = 5$ for circuit experiment, $P > 0.05$ (*28*)]. Comparing shoulder elevations during the exo and no exo conditions, we observed 8.7° and 4.6° angle increases for screw and wire tasks, respectively (paired *t* test for normal data and Wilcoxon's signed-rank test for non-normal data, $n = 5$, $P < 0.01$ for screw, $P < 0.05$ for wire), and no significant difference for the hold task (Fig. 4B). The observed increases are less than 5% of the shoulder elevation range of motion. For shoulder horizontal extension angle, no significant changes were observed among all tasks. For elbow angles, significant change was found during the holding task, with an increase of 6.7° ($P < 0.01$) when using the robot (Fig. 4B).

Controller accuracy during circuit task

We calculated the controller accuracy for each circuit task or transition among tasks. Overall, the controller had a higher true negative rate (TNR) (96.1%) than true positive rate (TPR) (91.3%) (Table 1), indicating that the controller is less likely to misinflate and impede the user when assistance is not needed than to misdeflate. Among the shoulder-elevated tasks, the controller was more consistent for the holding and screw tasks, with 92.0% and 93.0% TPR, respectively, and was least accurate for the wiring task, with 84.0% TPR (Table 1). Among the transition movements that did not require assistance, the controller did not interfere with the user during the task transitions or desk work (100% TNR) (Table 1). However, during task transitions and walking, the controller achieved a TNR of 95.5% and 95.8%, respectively (Table 1). For all misclassifications, the duration was brief (approximately less than 2 s for misinflations and less than 1.5 s for misdeflations) and did not occur over the entire duration of the task.

No increases in antagonistic LAT activation during arm lowering

During the arm-lowering phases across all experiments, with offset velocities (velocity at which the robot deflated; fig. S1C) ranging between −30°/s and −110°/s [adaptation based on (*20*) with approximately 4°/s root mean square error], we did not find any significant increases in the LAT mean and maximum activation when using the robot through group-level analysis (paired *t* test for normal data and Wilcoxon's signed-rank test for non-normal data, $n = 9$, 8, and 5 for holding, drilling, and circuit experiments, respectively, $P > 0.05$) (Fig. 5). A small increase in antagonist LAT activity [mean increase of up to 1% MVC (Fig. 5A)] was observed, but no statistical significance was found in the investigated sample sizes. Among all the tasks, drilling required the lowest mean LAT activation of 2 to 4% MVC during both no exo and exo conditions, whereas other tasks required an average activation of approximately 5 to 7% MVC (Fig. 5A). Further evaluations on weighted arm lowering with various fixed offset

Table 1. Controller performance during circuit task. The results were computed from five participants with five circuit task cycles per participant. n/a, not applicable.

	True negative rate	True positive rate
Tasks not requiring assistance		
All	96.1%	n/a
Transitions	95.5%	n/a
Desk work	100%	n/a
Walking	95.8%	n/a
Tasks requiring assistance		
All	n/a	91.3%
Hold	n/a	92.0%
Screw	n/a	93.0%
Wire	n/a	84.0%

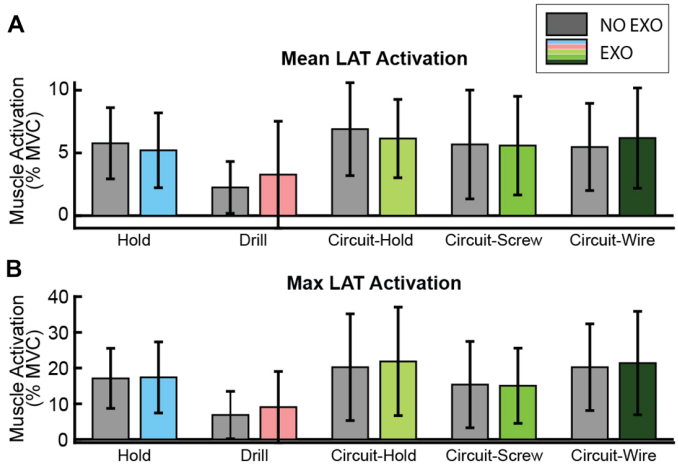

Fig. 5. LAT activation during the arm-lowering phases. (**A**) Averaged mean and (**B**) averaged peak LAT activation during arm lower phases across task repetitions of all experiments, with no significant differences observed between exo and no exo conditions [no significant differences ($P > 0.05$) were found with paired *t* test for comparing normal data and Wilcoxon's signed-rank test for comparing non-normal data, with normality determined by Shapiro-Wilk parametric hypothesis test, $n = 9$ for holding, $n = 8$ for drilling, $n = 5$ for circuit experiment]. The error bars represent SD across participants. For holding and drilling experiments, the exo condition data were averaged across all exo conditions of different assistance magnitudes and timings for each participant.

velocities (−80°/s to −30°/s) and actuator pressures (low, med, high) also showed minimal differences in the LAT activity (Supplementary Methods and fig. S4).

Pressure modulation improves perception

To further explore the capabilities of an active robot, we performed a preliminary demonstration of providing modulated pressure (Supplementary Methods and fig. S7) during a task involving holding and transitioning among three heights (Fig. 1E). We compared the modulated assistance (mod) with low and high conditions. We evaluated user perception and pump duty cycle in addition to changes in muscle activity.

The mod condition resulted in reductions in muscle activity (Fig. 6A) compared with no exo (only descriptive statistics were performed because of small sample size), with greater user preference compared with low and high constant pressure profiles (Fig. 6B). However, the pump duty cycle was increased when tracking the modulating pressure (Fig. 6C), resulting in a trade-off between hardware demand and user preference.

Industrial workers' feedback

Five workers used the robot at a production line prototyping area (performing the same tasks as in a real production line but at a slower pace) (Fig. 7). Users considered the robot helpful for static overhead tasks (such as holding objects) and less helpful for highly dynamic tasks. Some workers found the weight and comfort of the system to be acceptable, whereas others expressed the need for better fit and weight distribution. All participants agreed that the level of support was sufficient to hold their arms up without requiring any effort to maintain the position.

DISCUSSION

We demonstrated a fully portable soft active shoulder robot for industrial use that was capable of reducing muscle activity during drilling and holding tasks. We understood the effects of modifying assistance magnitude on EMG levels, with greater assistance resulting in greater mean EMG reductions with statistical significance. Furthermore, at

a group level across all tasks, we found no significant increases in the latissimus dorsi. Delayed actuator inflation resulted in fewer kinematic deviations from natural arm movements. The preliminary evaluation of a modulating pressure profile also unveiled a trade-off between hardware demands and user preference.

The proposed soft inflatable robot reduced muscle activity by up to 40% in the deltoids and up to 50% in the bicep brachii, in a similar range to the state of the art [16 to 73% (*8*)]. Specifically, these observations were made during the drilling and holding experiments, which have been commonly evaluated (*29*–*32*), and the tool weight and heights of work zones were comparable to previously evaluated ranges (0.4 to 8 kg, shoulder to overhead height). Additionally, workers reported that the level of support provided by the robot was enough to hold the weight of their arms, which enables the possibility of studying the effects of the robot in mitigating fatigue, as shown in previous work in the field (*33*, *34*). Compared with existing rigid devices that can provide a range of peak torques between 5 and 20 Nm (*10*, *35*–*37*) and soft devices applying torques between 4 and 11 Nm (*38*), our soft inflatable robot is capable of applying torque in a similar range (greater than 6 Nm; Supplementary Methods and figs. S5 and S6). We observed that the assistance applied was sufficient to achieve significant reductions in shoulder agonist muscle activities. We hypothesize that more EMG reductions may be achieved with higher torque outputs as shown in previous studies [up to 80% EMG reductions with 20 Nm peak torque (*10*) and up to 73% reductions from an exoskeleton applying 5- to 9-kg force at arm end (around 14 Nm for a 0.3-m moment arm) (*12*)]. Consistent with the hypothesis, we observed that significant reductions were achieved in the agonist muscles beyond certain assistance levels (exemplified by med and high in Fig. 2A). Moreover, the lack of change between the agonist muscle activities comparing the holding task performed in isolation with the hold performed as part of the circuit demonstrated the consistency of the approach despite different hold durations and tasks before the hold. Although small increases in shoulder elevation, horizontal extension, and elbow extension [less than 7% range of motion, considering 180° for shoulder elevation (*39*), horizontal flexion, and extension and 146° for elbow angle (*40*)] were found when using the robot, they were not associated with additional EMG increases. Additionally, although deltoid activity is expected to increase with increased shoulder elevation angles when unassisted, because deltoid muscles contribute to shoulder flexion and abduction (*41*, *42*), no increase in deltoid EMG was observed in this study.

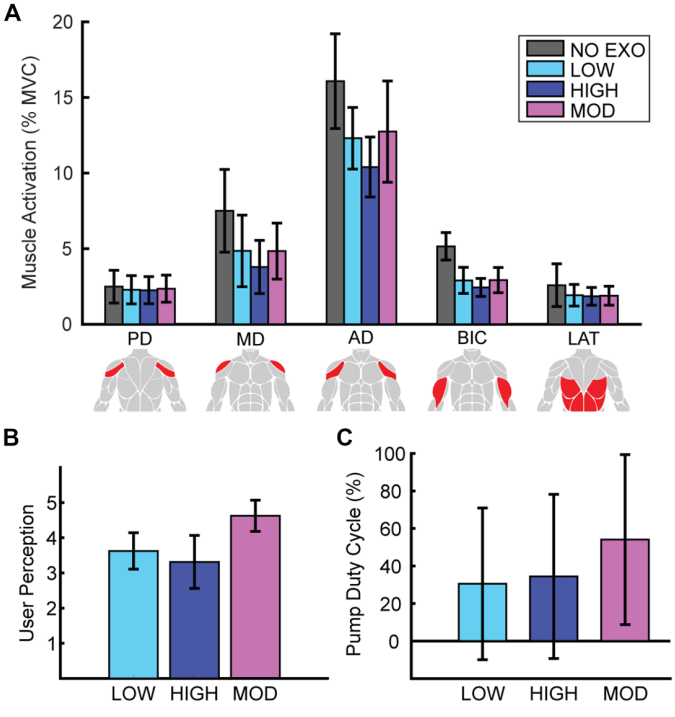

Fig. 6. Effects of modulating pressure profile. (**A**) Muscle activation in % MVC for no exo, low, high, and mod conditions for all muscle groups during the pressure modulation experiment involving a holding task at various heights [n = 40 (four participants, 10 repetitions)]. (**B**) User perception of the assistance conditions, with higher number indicating higher preference [n = 8 (four participants, two ratings)]. (**C**) Pump duty cycle during the assistance conditions [n = 40 (four participants, 10 repetitions)]. Descriptive statistics only because of small sample size; error bars represent SD across all repetitions among all trials for all participants.

Although a small increase in antagonist LAT activity was observed when lowering the arm, this was not statistically significant at a group level at the current sample size. This result contrasts with some studies with existing rigid passive devices, which found increases in the antagonistic muscles (*9*, *12*). However, this small but nonsignificant increase observed in LAT activity is consistent with previous findings for latissimus dorsi and erector spinae (*43*, *44*). Moreover, from interpolated time-series torque on two individuals (fig. S6), we observed an increase in torque during the arm-lowering phase before the actuator fully deflated (around 1 s in duration). These momentary resistive torques may explain the increased LAT activation observed for individual participants (Supplementary Materials). For individuals who did not experience an increase in LAT activity, the torque applied by the robot was comparable to the downward force applied to the arm by gravity. Although some variations in the individual response exist, our group analysis here on a small sample size did not result in significant LAT activity increase. Nonetheless, improvements in the control strategy and reductions in system pneumatic resistance would allow for faster actuator deflation, which will help to minimize the magnitude of this torque spike and will be considered for future work. Monitoring additional muscle groups (because changes could have occurred in other nonmonitored antagonistic groups) on a larger sample size would also allow further understanding and conclusions.

Moreover, because LAT activity was reduced during the holding task with exo conditions (Fig. 2A), we hypothesize that LAT was engaged for stabilization during the hold and that the robot provided support once powered on. Future studies will need to confirm this hypothesis. Significant reductions were found in BIC for the holding task. Although primarily responsible for elbow flexion, BIC is also a stabilizer during shoulder elevation (*24*) and was assisted by the robot.

During the circuit experiment, we demonstrated controller classification accuracy above 90% (Table 1), which is in the range of current intention detection methods using EMG and kinematics (*45*). Although accuracy was lower than our previous controller evaluation at three distinct heights (*20*), the experimental activities were more dynamic and varied in this work. Higher accuracy may be achieved using alternative methods to determine user intent, such as using machine learning with EMG (*46*, *47*); however, requiring training data was something we looked to avoid in this work.

In previous studies, the torque generated by the actuators has been shown to be linearly correlated with the inflation pressure both

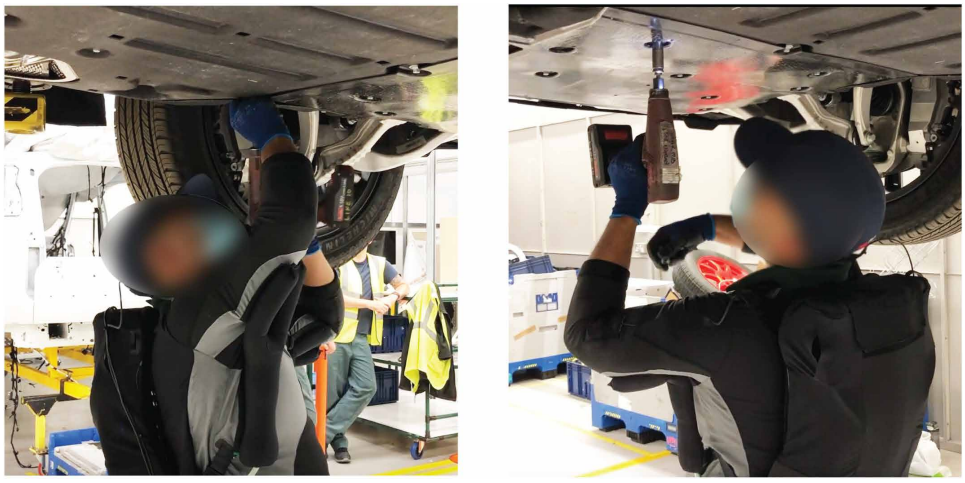

Fig. 7. Factory worker performing overhead tasks while assisted by the robot.

on the bench top (*15*, *22*) and in situ on the human body (*23*), and this trend may explain that higher actuator pressure allowed for statistically significant EMG reductions (Fig. 2A). Specifically, we assessed the torque outputs from the two actuator sizes used in the study (large and small size; fig. S1F). From interpolated torques during the holding task, we observed higher torque magnitudes for higher actuator pressures, with the large actuator providing 5.5 ± 1.3, 6.0 ± 1.5, and 6.6 ± 1.8 Nm (mean ± SD) for low, med, and high, respectively, and the small actuator providing 3.4 ± 1.0, 3.4 ± 1.9, and 3.5 ± 1.6 Nm, respectively (Supplementary Methods). Because no significant kinematic variations were observed (Fig. 2B) within this estimated range of torques, more EMG reductions, without additional kinematic deviations, may have been possible if higher actuator pressures were applied. However, because there exist trade-offs between pressure and comfort (*48*), as well as the fluidic system requirements, actuator pressure may not be increased unboundedly without these considerations.

Similar to previous findings (*29*, *32*, *33*, *49*), changes in kinematics were observed, including increased shoulder elevation (*49*, *50*). However, there is limited understanding on the effect of these changes. As noted by the US Consumer Product Safety Commission (CPSC), muscle strain may be caused if active exoskeletons move a user's joints beyond their natural ranges of motion (*51*). However, the kinematic changes observed in this study (less than 12°) are in line with previous research and within the natural range. Although negative effects have not been reported with short-term exoskeleton use that causes such kinematic changes, the longer-term effect on user ergonomics should be further investigated.

Given that early inflation resulted in significant EMG reduction (Fig. 3A), more lateral elbow motion (Fig. 3C), and changes in joint angles (Fig. 3B), the optimal inflation time is dependent on whether such trajectory deviation while assisted has negative biomechanical effects, which remains to be better understood. Moreover, early inflation through a lower onset angle may result in a lower TNR (causing misinflations at low arm elevation), creating a trade-off between controller accuracy and providing early assistance. In practice, we hypothesize that for industrial tasks requiring longer durations, small differences in assistance timing (inflating approximately 300 ms later for around 20° of higher onset angle in this study) will not substantially affect the overall benefit of the robot because it is a small percentage of total task time.

Even with the simplicity of constant controller parameters, this study helped with elucidating design considerations for providing active assistance with inflatable soft robots. The constant pressure profile together with the compliance of the inflatable actuator enabled assistance (reduced muscle activity and user perception of support) during quasi-static tasks. Additionally, for dynamic tasks, active robots have the potential to provide adaptive assistance and are more likely to avoid the trade-off between increased assistance and discomfort and the need to select an optimal setting, which are characteristics of passive devices (*8*, *14*). However, more adaptive controllers also impose higher demands on system hardware (Fig. 6C), which are associated with higher system weight and noise and shorter battery life. Hence, a trade-off between controller adaptability and hardware requirements exists, and the optimal level of adaptability may be determined through the use case.

The evaluation of the soft active wearable robot showed promise for reducing agonist muscle activity without increasing antagonistic muscle activity. The laboratory-based study is a step toward elucidating the effects of assistance timing and magnitude on user biomechanics and the range of assistance that can be provided by a soft active robot. Qualitative feedback from industrial workers also built confidence for using such a robot in unconstrained assembly environments. However, the system controller, which triggers at a fixed onset angle and a set actuator pressure, limited their perception of its suitability for more dynamic tasks. Because the current study is limited by the small sample size, in future work, we aim to expand evaluations for more individuals. Additionally, the individualized actuator pressure chosen by the participants in this study may have been conservative, especially for screw and wire tasks involving higher elevation angles (fig. S2), given that the torque applied decreases with elevation angle (fig. S5). Moreover, although the controller (*20*) aimed to balance ease of deflation with the risk of misdeflations for tasks of various speeds, some misdeflations still occurred during high-velocity motions. Further controller development could incorporate task classification to identify which tasks require faster speeds and adjust velocity thresholds accordingly. Because an increased pump duty cycle was found during pressure modulation (Fig. 6C), future hardware improvements are also necessary to reduce pump duty cycle and improve battery life. This research motivates additional development and longer duration quantitative studies in the real world to further validate robot usability and biomechanical effects.

MATERIALS AND METHODS

Objective and design

The objective of the study was to design and evaluate the performance of a soft inflatable shoulder robot for assisting industrial work during controlled and dynamic tasks. The experiment was designed to

measure muscle activity and joint kinematics and positions during a range of robot assistance conditions to evaluate the effect of the robot on user biomechanics. All conditions were assessed during simulated industrial tasks or motions and common tasks that do not require assistance in the work scenario.

Soft inflatable shoulder robot

The soft inflatable shoulder robot (Fig. 1A and fig. S1) consisted of two actuators (fig. S1F), three IMUs, and a portable actuation unit (fig. S1A) all integrated into functional apparel (fig. S1E). In collaboration with our industry partner, we identified that, on average, workers typically perform shoulder-elevated tasks six times per minute during certain parts of automotive assembly. In addition, although tool weight varied, we set a requirement of supporting up to 2.3 kg of weight (an external tool, such as a drill) in each hand. It was also deemed important that the robot should not weigh more than 4 kg (to allow for extended usage) and be able to assist quickly (within 2 s of an individual beginning a task).

Actuator

The actuator design was based on our previous works (*13*, *16*, *20*–*22*). Actuators were fabricated with an inextensible textile shell (Typhoon 65% polyester, 35% cotton, Milliken & Company, USA) enclosing an inflated TPU bladder (TPU hot melt adhesive film, PerfectTex, USA) and were patterned with a bifurcated shape designed to provide a torque about the shoulder when inflated. Using average anatomical upper extremity lengths (*26*) expressed in percentage body height (*27*), the biological torque required to support 2.3 kg at 90° shoulder and elbow flexion was estimated to be 6.5 Nm (Supplementary Methods). Through iterative design for the large-size actuator (fig. S1F), we set the actuator volume to 0.64 liter. The actuator produced the target 6.5 Nm of torque when inflated to 70 kPa at 90° under benchtop conditions. This was based on previous benchtop characterizations that showed strong correlation between torque output and actuator pressures and volumes (*22*, *23*). However, higher pressures and volumes corresponded to greater fluidic demands on the portable actuation unit and increased risk of material failures. Lastly, although we had a requirement of 70 kPa, this target pressure was based on average anthropometrics, and we expected individualized pressure to be more suitable for each user to account for different body proportions. Hence, we set a range of operating pressures from 65 to 100 kPa. To accommodate smaller body sizes, we developed a scaled-down actuator (small size in fig. S1F) and applied the same range of operating pressures.

Portable actuation unit

The custom-designed portable actuation unit contained an accumulator (compressed air reservoir), a pump, and two sets of solenoid valves (fig. S1, A and B). Three analog pressure sensors were placed in line with the accumulator and actuators, and all components were connected through flexible tubing.

The components of the actuation unit were chosen to meet the fluidic demand of supporting both arms six times per minute at a maximum actuator operating pressure of 100 kPa. The pump flow must match or exceed the actuation unit's average rate of consumption. Following previous work on pneumatic system optimization (*52*), under normal flow conditions, this relationship is defined as

$$Q = \frac{R \times V_{act} \times P_0}{P_{atm}} \quad (1)$$

where Q is the average pump flow, R is the actuation frequency, V_{act} is the total actuator volume, P_0 is the actuator operating pressure, and P_{atm} is atmospheric pressure. The estimated fluidic demand of the actuation unit was 15.3 liters per minute. A single piston pump (ASPINA, Shinano Kenshi Corporation, Japan) was selected, meeting these demands while weighing only 430 g. The accumulator was included to allow for on-demand fast inflation of the actuators. Its storage capacity was the product of its volume and pressure, with the latter capped by the chosen pump maximum pressure (207 kPa for the chosen pump). Storage capacity was designed to ensure that the accumulator stores enough air to maintain a negative pressure gradient throughout actuator inflation. To have sufficient storage capacity, the accumulator volume (V_{ac}) must satisfy

$$V_{ac} \geq \frac{P_0 \times V_{act} - Q_{ave} \times T \times P_{atm}}{P_{max} - P_0} \quad (2)$$

where T is the intended inflation time, P_{max} is the maximum accumulator pressure, and Q_{ave} is the average pump flow during inflation, following (*52*). As a result, the accumulator required a minimum volume of 1.47 liters. Two 0.83-liter aluminum cans (Crowler Nation, USA) were chosen as a lightweight solution. Finally, four solenoid valves (Nitra pneumatics, AutomationDirect, USA) with a valve flow coefficient of 0.5 were selected as sufficient to meet the target inflation time. The portable actuation unit was powered by two swappable batteries (standard battery pack RRC2054, RRC power solutions GmbH, Germany) capable of approximately 1.5 hours of continuous use at six cycles per minute inflation frequency (about 540 inflations). The total weight of the portable actuation unit with all electromechanical components was 3.4 kg, assembled in a custom structural box with dimensions 28 cm by 9 cm by 40 cm.

Apparel

The functional apparel was composed of several textile materials, patterned for loading path, breathability, and flexibility. Woven textiles (twill/plain) were used to react forces from the actuator and hold the actuator close to the body [fig. S1E, i and ii (gray regions)]. Adjustment webbing acted as high-tension loading paths and were used to connect the apparel to the actuation unit and support its weight [fig. S1E, iii (black with red border)]. The actuation unit was placed in a hiking backpack–style frame, with a breathable spacer mesh interfacing against the user's back (fig. S1E, iv). The apparel integrated the actuators, actuation unit, sensing, and control components into one standalone device, allowing for short donning and doffing time of approximately 30 and 14 s, respectively, for an experienced user (fig. S1H).

Sensing and control

Three IMUs, two placed on the upper arms in the IMU sleeve pockets (fig. S1E) and one in the actuation unit (which coupled with trunk motion) (fig. S1A), were used to estimate shoulder kinematics. The shoulder elevation angle was estimated from the orientation of the arm IMU in the frame of the trunk IMU. A calibration was conducted while the users stood straight with arms by their sides to minimize sensor-to-segment misalignment. The kinematics-based state-machine controller (*20*) determined inflation and deflation states using threshold crossings of elevation angle and elevation velocity when the trunk is upright. Specifically, onset angle (θ_{on}) is the elevation angle at which the controller transitions from a deflated to an inflated state, and the offset angle (θ_{off}) and offset velocity ($\dot{\theta}_{off}$) are the elevation angle and velocity at which the controller transitions from inflated to deflated, respectively (fig. S1C). In the inflated

state, the controller commanded a constant pressure (except for mod condition), and the command pressure was maintained through a bang-bang low-level controller (fig. S1D). Because of the use of solenoid valves, a maximum overshoot of 6.9 kPa was allowed when inflating the actuator. When holding at the inflated state, the valves reopened to fill the actuator when the pressure dropped below 90% of the commanded pressure. The accumulator pressure was controlled between a maximum pressure of 241 kPa and a minimum pressure of 207 kPa. To reduce pump duty cycle, noise, and system temperature, the pump was turned on only when the accumulator pressure dropped below the minimum pressure and filled the accumulator until the maximum pressure.

Experimental methods

We recruited 14 participants in total across all experiments. Data for some trials were not included in the analysis because of technical and procedural issues [errors in onset angle (mean IMU-estimated angle more than 5° from intended), inconsistency in pressure delivered (pressure outside of the actuator intended operating range or high deviation from selected P^* due to wrong sensor readings)] or inability to complete the study. We analyzed the data for nine participants for holding, eight for drilling, five for the circuit task, and four for the pressure modulation experiment. The study (IRB19-1321) was approved by the Harvard Medical School Institutional Review Board (HMS-IRB), and each participant gave informed consent before participation. For torque evaluations, because of the focus on actuator response, the HMS-IRB determined that portion of the testing to be Not Human Subject Research (NHSR).

To account for body-size variations, each participant selected a pressure P^* in the range of 65 to 100 kPa on the basis of comfort and perceived support during arm flexion without holding any weight using actuators scaled to shirt sizes (two actuator sizes; fig. S1F). P^* was used as an individualized reference assistance level in all experiments. Different P^* values were possible for experiments on different days. The resulting measured mean P^* across all participants was 78.5 ± 10.3 kPa.

For all experiments, muscle activation was captured with wireless surface EMG sensors (Delsys, Natick, MA, USA), and MVCs were collected with four exercises: lateral shoulder raise, forward shoulder raise, biceps brachii curls, and lateral shoulder push-downs. User kinematics were measured through a motion capture system (Qualisys Motion Capture Systems, Gothenburg, Sweden).

In the holding experiment (Fig. 1B), the order of no exo and exo conditions was randomized among the participants to avoid bias in results due to fatigue (order within the exo conditions remained the same). The pressure increments of 16 kPa were chosen because they were generally differentiable through user perception. In the drilling experiment (Fig. 1C), the participants were asked to lower their arms between drilling cycles to allow multiple repetitions of the arm-raising and targeting motion, with the last three complete drilling out repetitions analyzed. The weight of the drill was 1.6 kg. The bolt height was individualized such that each participant elevated their arm at approximately 80° when drilling. For consistency, all participants were instructed to use their right hand.

For the circuit experiment task heights, the holding task was at each participant's eye level. The screw task involved four targets requiring between approximately 80° and 90° shoulder elevation. The wiring task required approximately 100° of shoulder elevation. On the basis of past work characterizing actuator mechanics (*22*), we hypothesized that the robot would be more assistive at lower working angles and reduced EMG for the holding task. For the screw and wire tasks at higher elevation angles, we aimed to test whether the robot would be unrestrictive during dynamic tasks at higher heights. The tasks not requiring assistance and transitions were also used to assess the controller's ability to assist when needed and not impede otherwise. The order of no exo and exo conditions was randomized among participants to minimize fatigue and learning effects. Each condition containing five cycles required approximately 10 min. During the exo condition, the command pressure was P^* (to evaluate user choice on the basis of perception), and the onset angle was 55°, which was the same condition as the low assistance magnitude during holding experiment and mid assistance timing during drilling experiment.

For the preliminary evaluation of pressure modulation compared with constant pressure profiles, the modulated pressure profile (mod) was designed via a calibration process mapping IMU-based shoulder elevation angle to actuator pressures, similar to previous work (*15*) (Supplementary Methods and fig. S7A). During all conditions (no exo, low, high, and mod), the participants held a 1.6-kg weight while targeting among three heights at approximately 70%, 77.5%, and 85% of body height following a 60–beats per minute (BPM) metronome. The right (and dominant) side was used by all participants. The participants performed the no exo condition twice first, followed by a 5-min rest or until the participant was ready. Afterward, exo conditions of low, high, and mod in randomized orders were performed, with each condition performed twice (Fig. 1E). The participants rated each exo condition on the scale of one to five (with higher values indicating higher preference). The onset angle was between 20° and 30°, and offset velocity was at −99°/s to allow early inflation and maximize range of pressure modulation.

For all experiments, we did not enforce specific posture with regard to the elbow angle but intended for the elbow angles to be around 90° flexion for holding, drilling, and circuit experiments and around 90° to 135° for pressure modulation experiments. During circuit experiments, outside of the bilateral tasks, all participants could perform each task with the preferred side. The participants rested for at least 2 min between the conditions and 5 min between the experiments. For the controller parameters, unless specified in the experiment condition, the onset angle was within 45° to 55°, offset angle was 50°, and the starting offset velocity was between −70°/s and −30°/s, because these values were found to be suitable during preliminary testing. The offset velocity adapted during the duration of the study was as in (*20*), allowing for the different offset velocities for each experimental trial, task cycle, and user to simulate real-world use.

Feedback from industry workers

Five factory workers [five males with height 1.76 ± 0.07 m (mean ± SD); table S2] used the robot at a pilot manufacturing area on site with our industrial partner. The workers wore the robot for approximately 30 min each (Fig. 7). They performed the same tasks as in a real production line, except without time constraints. To allow for unsupervised use, the users self-selected the actuator-commanded pressure among 55, 69, and 83 kPa. The onset angle (fig. S1C) was fixed at 55° as selected from test use cases in the laboratory. The workers' feedback was collected as a group because of critical time constraints derived from the production line. This feedback provides a sense of the preliminary impressions of industrial workers using this technology.

Analysis of data

EMG processing

A standard EMG filter was applied following our previous work (*13*): first, a fourth-order band-pass filter between 10 and 400 Hz, then signal rectification, and finally a fourth-order low pass filter at 10-Hz cutoff frequency. The EMG raw signal was sampled at 2 kHz (2.148 kHz for pressure modulation experiments). Muscle groups from both sides of the body were analyzed for the holding experiment. For the unilateral drilling experiment, the right-side muscles were used and analyzed. For the circuit experiment, muscle groups from the dominant side of the body were analyzed.

Kinematics processing

To evaluate the joint trajectories independently of variable participant body sizes, we normalized the upper and forearm lengths to 29.03 and 26.67 cm, respectively, following average anthropometric data (*26*, *27*). For joint angles, shoulder elevation angles were computed by comparing the upper arm longitudinal axis with gravity. Shoulder horizontal extension angles were computed comparing the longitudinal axis of the upper arm (projected on the horizontal plane) with the trunk sagittal axis (anterior direction defined by bilateral shoulder positions). Elbow angles were computed as the angles between the upper arm longitudinal axis and the axis connecting the elbow and wrist joint centers (with 180° defined as fully extended).

Circuit experiment analysis

To evaluate the controller, we computed TPR and TNR of the controller classification. TPR was defined as the ratio of true positives to the total number of positives (the number of tasks requiring assistance: hold, screw, wire); TNR was defined as the ratio of true negatives to the total number of negatives (the number of transitions and tasks not requiring assistance: walk, desk work). Mismatches between the exact starts and ends of labeled and classified states were allowed to account for segmentation imperfections and controller response time (mean mismatch of approximately 0.6 s). Five cycles of the circuit tasks were performed in each condition, and the last four cycles were analyzed for EMG (to compare the same number of installation and removal motions) (except one participant, for whom we used the first four cycles because of incompletion), whereas all five cycles were analyzed for controller evaluation (to maximize the total number of motions assessed disregarding directionality).

Statistical analysis

For statistical analysis of the mean EMG and joint angles for drilling and holding experiments, we applied Friedman's test with Tukey-Kramer post hoc analysis for each of the three repetitions of drilling and holding tasks during each condition (segmentation and repetition details in Supplementary Methods). Because of missing holding kinematics data for one repetition from one participant, the holding task kinematics were analyzed with two hold repetitions for each participant. For EMG and joint angle measurements of the circuit task, we first evaluated the normality of the data using the Shapiro-Wilk parametric hypothesis test with a significance level of 0.05 with implementation by (*53*). For normal data and non-normal data, we applied paired *t* tests and Wilcoxon's signed-rank tests, respectively, to compare the mean EMG measurements and joint angles between the exo and no exo condition for each participant (not accounting for each cycle as a repeated measure). For analysis of LAT activation during arm lowering, the various exo conditions for drilling and holding experiments were averaged to consider one mean value for exo condition per participant. Descriptive statistics were applied to the pressure modulation experiment.

Supplementary Materials

This PDF file includes:

Methods
Figs. S1 to S7
Tables S1 and S2
Reference (*53*)

Other Supplementary Material for this manuscript includes the following:

Data file S1
MDAR Reproducibility Checklist

REFERENCES AND NOTES

1. Centers for Disease Control and Prevention, Work-related musculoskeletal disorders & ergonomics (2020); https://www.cdc.gov/workplacehealthpromotion/health-strategies/musculoskeletal-disorders/index.html.
2. Ford Media Center, "Ford rolls out exoskeleton wearable technology globally to help lessen worker fatigue, injury," 7 August 2018; https://media.ford.com/content/fordmedia/fna/us/en/news/2018/08/07/ford-rolls-out-exoskeleton-wearable-technology-globally-to-help-html.
3. US Bureau of Labor Statistics, Injuries, illnesses, and fatalities (2020); https://www.bls.gov/iif/nonfatal-injuries-and-illnesses-tables/case-and-demographic-characteristics-table-r2-2020.htm.
4. US Bureau of Labor Statistics, MSD by part of body affected by days away from work (number, rate, median) (2023); https://www.bls.gov/iif/nonfatal-injuries-and-illnesses-tables/soii-case-and-demographic-characteristics-historical-data/msd-case-and-demographic-part-of-body-2020-national.xlsx.
5. P. Maurice, J. Camernik, D. Gorjan, B. Schirrmeister, J. Bornmann, L. Tagliapietra, C. Latella, D. Pucci, L. Fritzsche, S. Ivaldi, J. Babic, Objective and subjective effects of a passive exoskeleton on overhead work. *IEEE Trans. Neural Syst. Rehabil. Eng.* **28**, 152–164 (2020).
6. I. Pacifico, A. Scano, E. Guanziroli, M. Moise, L. Morelli, A. Chiavenna, D. Romo, S. Spada, G. Colombina, F. Molteni, F. Giovacchini, N. Vitiello, S. Crea, An experimental evaluation of the Proto-MATE: A novel ergonomic upper-limb exoskeleton to reduce workers' physical strain. *IEEE Robot. Autom. Mag.* **27**, 54–65 (2020).
7. E. Rashedi, S. Kim, M. A. Nussbaum, M. J. Agnew, Ergonomic evaluation of a wearable assistive device for overhead work. *Ergonomics* **57**, 1864–1874 (2014).
8. A. de Vries, M. de Looze, The effect of arm support exoskeletons in realistic work activities: A review study. *J. Ergon.* **9**, 1–9 (2019).
9. L. Van Engelhoven, N. Poon, H. Kazerooni, D. Rempel, A. Barr, C. Harris-Adamson, Experimental evaluation of a shoulder-support exoskeleton for overhead work: Influences of peak torque amplitude, task, and tool mass. *IISE Trans. Occup. Ergon. Hum. Factors* **7**, 250–263 (2019).
10. L. Van Engelhoven, N. Poon, H. Kazerooni, A. Barr, D. Rempel, C. Harris-Adamson, Evaluation of an adjustable support shoulder exoskeleton on static and dynamic overhead tasks. *Proc. Hum. Factors Ergon. Soc. Annu. Meet.* **62**, 804–808 (2018).
11. J. Howard, V. V. Murashov, B. D. Lowe, M. Lu, Industrial exoskeletons: Need for intervention effectiveness research. *Am. J. Ind. Med.* **63**, 201–208 (2020).
12. J. Theurel, K. Desbrosses, T. Roux, A. Savescu, Physiological consequences of using an upper limb exoskeleton during manual handling tasks. *Appl. Ergon.* **67**, 211–217 (2018).
13. T. Proietti, C. O'Neill, C. J. Hohimer, K. Nuckols, M. E. Clarke, Y. M. Zhou, D. J. Lin, C. J. Walsh, Sensing and control of a multi-joint soft wearable robot for upper-limb assistance and rehabilitation. *IEEE Robot. Autom. Lett.* **6**, 2381–2388 (2021).
14. S. Kim, S. Madinei, M. M. Alemi, D. Srinivasan, M. A. Nussbaum, Assessing the potential for "undesired" effects of passive back-support exoskeleton use during a simulated manual assembly task: Muscle activity, posture, balance, discomfort, and usability. *Appl. Ergon.* **89**, 103194 (2020).
15. T. Proietti, C. O'Neill, L. Gerez, T. Cole, S. Mendelowitz, K. Nuckols, C. Hohimer, D. Lin, S. Paganoni, C. Walsh, Restoring arm function with a soft robotic wearable for individuals with amyotrophic lateral sclerosis. *Sci. Transl. Med.* **15**, eadd1504 (2023).
16. C. T. O'Neill, N. S. Phipps, L. Cappello, S. Paganoni, C. J. Walsh, A soft wearable robot for the shoulder: Design, characterization, and preliminary testing, in *2017 International Conference on Rehabilitation Robotics (ICORR)* (IEEE, 2017), pp. 1672–1678.
17. C. S. Simpson, A. M. Okamura, E. W. Hawkes, Exomuscle: An inflatable device for shoulder abduction support, in *2017 IEEE International Conference on Robotics and Automation (ICRA)* (IEEE, 2017), pp. 6651–6657.
18. A.-M. Georgarakis, M. Xiloyannis, P. Wolf, R. Riener, A textile exomuscle that assists the shoulder during functional movements for everyday life. *Nat. Mach. Intell.* **4**, 574–582 (2022).
19. E. Bardi, M. Gandolla, F. Braghin, F. Resta, A. L. G. Pedrocchi, E. Ambrosini, Upper limb soft robotic wearable devices: A systematic review. *J. Neuroeng. Rehabil.* **19**, 87 (2022).
20. Y. M. Zhou, C. Hohimer, T. Proietti, C. T. O'Neill, C. J. Walsh, Kinematics-based control of an inflatable soft wearable robot for assisting the shoulder of industrial workers. *IEEE Robot. Autom. Lett.* **6**, 2155–2162 (2021).

21. C. O'Neill, T. Proietti, K. Nuckols, M. E. Clarke, C. J. Hohimer, A. Cloutier, D. J. Lin, C. J. Walsh, Inflatable soft wearable robot for reducing therapist fatigue during upper extremity rehabilitation in severe stroke. *IEEE Robot. Autom. Lett.* **5**, 3899–3906 (2020).
22. C. T. O'Neill, C. M. McCann, C. J. Hohimer, K. Bertoldi, C. J. Walsh, Unfolding textile-based pneumatic actuators for wearable applications. *Soft Robot.* **9**, 163–172 (2022).
23. C. M. McCann, C. J. Hohimer, C. T. O'Neill, H. T. Young, K. Bertoldi, C. J. Walsh, In-situ measurement of multi-axis torques applied by wearable soft robots for shoulder assistance. *IEEE Trans. Med. Robot. Bionics* **5**, 363–374 (2023).
24. D. Landin, J. Myers, M. Thompson, R. Castle, J. Porter, The role of the biceps brachii in shoulder elevation. *J. Electromyogr. Kinesiol.* **18**, 270–275 (2008).
25. N. Bogduk, G. Johnson, D. Spalding, The morphology and biomechanics of latissimus dorsi. *Clin. Biomech.* **13**, 377–385 (1998).
26. S. Plagenhoef, F. G. Evans, T. Abdelnour, Anatomical data for analyzing human motion. *Res. Q. Exerc. Sport* **54**, 169–178 (1983).
27. C. D. Fryar, M. D. Carroll, Q. Gu, J. Afful, C. L. Ogden, "Anthropometric Reference Data for Children and Adults: United States, 2015–2018," Vital and Health Statistics, Series 3, Analytical and Epidemiological Studies, no. 46, report ID 100478 (US Department Of Health and Human Services, 2021).
28. G. Cardillo, MWWTEST: Mann-Whitney-Wilcoxon non parametric test for two unpaired samples (2009); http://www.mathworks.com/matlabcentral/fileexchange/25830.
29. S. Alabdulkarim, M. A. Nussbaum, Influences of different exoskeleton designs and tool mass on physical demands and performance in a simulated overhead drilling task. *Appl. Ergon.* **74**, 55–66 (2019).
30. S. Spada, L. Ghibaudo, C. Carnazzo, L. Gastaldi, M. P. Cavatorta, Passive upper limb exoskeletons: An experimental campaign with workers, in *Proceedings of the 20th Congress of the International Ergonomics Association (IEA 2018)*, S. Bagnara, R. Tartaglia, S. Albolino, T. Alexander, Y. Fujita, Eds., vol. 825 of *Advances in Intelligent Systems and Computing* (Springer International Publishing, 2019), pp. 230–239.
31. S. Kim, M. A. Nussbaum, M. I. Mokhlespour Esfahani, M. M. Alemi, S. Alabdulkarim, E. Rashedi, Assessing the influence of a passive, upper extremity exoskeletal vest for tasks requiring arm elevation: Part I—"Expected" effects on discomfort, shoulder muscle activity, and work task performance. *Appl. Ergon.* **70**, 315–322 (2018).
32. S. Kim, M. A. Nussbaum, M. I. Mokhlespour Esfahani, M. M. Alemi, B. Jia, E. Rashedi, Assessing the influence of a passive, upper extremity exoskeletal vest for tasks requiring arm elevation: Part II—"Unexpected" effects on shoulder motion, balance, and spine loading. *Appl. Ergon.* **70**, 323–330 (2018).
33. S. De Bock, T. Ampe, M. Rossini, B. Tassignon, D. Lefeber, C. Rodriguez-Guerrero, B. Roelands, J. Geeroms, R. Meeusen, K. De Pauw, Passive shoulder exoskeleton support partially mitigates fatigue-induced effects in overhead work. *Appl. Ergon.* **106**, 103903 (2023).
34. E. P. Lamers, J. C. Soltys, K. L. Scherpereel, A. J. Yang, K. E. Zelik, Low-profile elastic exosuit reduces back muscle fatigue. *Sci. Rep.* **10**, 15958 (2020).
35. L. Grazi, E. Trigili, N. Caloi, G. Ramella, F. Giovacchini, N. Vitiello, S. Crea, Kinematics-based adaptive assistance of a semi-passive upper-limb exoskeleton for workers in static and dynamic tasks. *IEEE Robot. Autom. Lett.* **7**, 8675–8682 (2022).
36. S. De Bock, J. Ghillebert, R. Govaerts, S. A. Elprama, U. Marusic, B. Serrien, A. Jacobs, J. Geeroms, R. Meeusen, K. De Pauw, Passive shoulder exoskeletons: More effective in the lab than in the field? *IEEE Trans. Neural Syst. Rehabil. Eng.* **29**, 173–183 (2021).
37. S. Ding, A. Reyes Francisco, T. Li, H. Yu, A novel passive shoulder exoskeleton for assisting overhead work. *Wearable Technol.* **4**, e7 (2023).
38. R. F. Natividad, T. Miller-Jackson, R. Y. Chen-Hua, A 2-DOF shoulder exosuit driven by modular, pneumatic, fabric actuators. *IEEE Trans. Med. Robot. Bionics* **3**, 166–178 (2020).
39. American Academy of Orthopaedic Surgeons, *Joint Motion: Method of Measuring and Recording* (Churchill Livingstone, 1965).
40. E. L. Zwerus, N. W. Willigenburg, V. A. Scholtes, M. P. Somford, D. Eygendaal, M. P. Van Den Bekerom, Normative values and affecting factors for the elbow range of motion. *Shoulder Elbow* **11**, 215–224 (2019).
41. A. Hecker, J. Aguirre, U. Eichenberger, J. Rosner, M. Schubert, R. Sutter, K. Wieser, S. Bouaicha, Deltoid muscle contribution to shoulder flexion and abduction strength: An experimental approach. *J. Shoulder Elbow Surg.* **30**, e60–e68 (2021).
42. R. F. Escamilla, K. Yamashiro, L. Paulos, J. R. Andrews, Shoulder muscle activity and function in common shoulder rehabilitation exercises. *Sports Med.* **39**, 663–685 (2009).
43. S. Iranzo, A. Piedrabuena, D. Iordanov, U. Martinez-Iranzo, J.-M. Belda-Lois, Ergonomics assessment of passive upper-limb exoskeletons in an automotive assembly plant. *Appl. Ergon.* **87**, 103120 (2020).
44. K. Huysamen, T. Bosch, M. De Looze, K. S. Stadler, E. Graf, L. W. O'Sullivan, Evaluation of a passive exoskeleton for static upper limb activities. *Appl. Ergon.* **70**, 148–155 (2018).
45. J. Russell, J. Bergmann, A systematic literature review of intent sensing for control of medical devices. *IEEE Trans. Med. Robot. Bionics* **4**, 118–129 (2022).
46. Y. Chen, Z. Yang, Y. Wen, A soft exoskeleton glove for hand bilateral training via surface EMG. *Sensors* **21**, 578 (2021).
47. H. C. Siu, A. M. Arenas, T. Sun, L. A. Stirling, Implementation of a surface electromyography-based upper extremity exoskeleton controller using learning from demonstration. *Sensors* **18**, 467 (2018).
48. J. Nassour, G. Zhao, M. Grimmer, Soft pneumatic elbow exoskeleton reduces the muscle activity, metabolic cost and fatigue during holding and carrying of loads. *Sci. Rep.* **11**, 12556 (2021).
49. T. Schmalz, J. Schändlinger, M. Schuler, J. Bornmann, B. Schirrmeister, A. Kannenberg, M. Ernst, Biomechanical and metabolic effectiveness of an industrial exoskeleton for overhead work. *Int. J. Environ. Res. Public Health* **16**, 4792 (2019).
50. T. C. McFarland, A. C. McDonald, R. L. Whittaker, J. P. Callaghan, C. R. Dickerson, Level of exoskeleton support influences shoulder elevation, external rotation and forearm pronation during simulated work tasks in females. *Appl. Ergon.* **98**, 103591 (2022).
51. Consumer Product Safety Commission, "Potential hazards associated with emerging and future technologies," staff report, 18 January 2017; https://www.cpsc.gov/s3fs-public/Report%20on%20Emerging%20Consumer%20Products%20and%20Technologies_FINAL.pdf.
52. S. Joshi, J. Paik, Pneumatic supply system parameter optimization for soft actuators. *Soft Robot.* **8**, 152–163 (2021).
53. A. BenSaïda, Shapiro-Wilk and Shapiro-Francia normality tests, version 1.1.0.0; https://www.mathworks.com/matlabcentral/fileexchange/13964-shapiro-wilk-and-shapiro-francia-normality-tests.
54. M. Sardelli, R. Z. Tashjian, B. A. MacWilliams, Functional elbow range of motion for contemporary tasks. *J. Bone Joint Surg. Am.* **93**, 471–477 (2011).

Acknowledgments: We thank E. Mann, J. Crystal, P. Banzet, J. Foster, B. Cohen, A. Chin, K. Swaminathan, C. Lee, S. Sullivan, and the clinical research team at Harvard University for their assistance during preparation and execution of the study. We thank our participants for their time toward this study. **Funding:** This research was supported by Tata Sons Private Limited and Jaguar Land Rover (C.J.W.), National Science Foundation [DGE1745303 (C.M.M. and H.T.Y.), EFRI #1830896 (C.J.W.), and MRSEC DMR2011754)], Office of Naval Research award no. N00014-17-1-2121 (C.J.W.), and Harvard School of Engineering and Applied Sciences (C.J.W.).
Author contributions: Conceptualization: Y.M.Z., C.J.H., H.T.Y., P.M., D.W., T.C., N.P., C.M.M., Y.J., H.C., T.P., and C.J.W. Methodology: Y.M.Z., C.J.H., H.T.Y., D.P.-E., U.S.C., P.M., D.W., T.C., H.C., and C.J.W. Investigation: Y.M.Z., C.J.H., D.P.-E., U.S.C., P.M., H.T.Y., D.W., T.C., F.B., and C.J.W. Analysis: Y.M.Z., C.J.H., C.M.M., and I.P. Visualization: Y.M.Z., C.J.H., C.M.M., and H.T.Y. Funding acquisition: C.J.W., C.M.M., and H.T.Y. Project administration: C.J.H., D.P.-E., and C.J.W. Supervision: C.J.W. Writing—original draft: Y.M.Z., C.J.H., H.T.Y., T.C., and C.J.W. Writing—review and editing: Y.M.Z., H.T.Y., T.P., Y.J., C.M.M., D.P.-E., and C.J.W. **Competing interests:** C.J.W. and N.P. are co-inventors on US Patent application US2022047444A1 filed by Harvard University that describes the inflatable soft robotic components tested in this study. The other authors declare that they have no competing interests. **Data and materials availability:** All data needed to support the conclusions of this manuscript are included in the main text or Supplementary Materials. Data and code can also be found on Zenodo: https://zenodo.org/records/11199453.

Submitted 12 April 2023
Accepted 17 May 2024
Published 12 June 2024
10.1126/scirobotics.adi2377